

FAST THERMAL ANALYSIS FOR VLSI CIRCUITS VIA SEMI-ANALYTICAL GREEN'S FUNCTION IN MULTI-LAYER MATERIALS

Baohua Wang and Pinaki Mazumder

Department of Electrical Engineering and Computer Science
The University of Michigan
Ann Arbor, Michigan, 48109, USA
Email: {baohuaw, mazum} @eecs.umich.edu

ABSTRACT

In this paper, we present a novel thermal analysis method for VLSI circuits based on the Green's function of heat conduction problem. Our approach can calculate the temperature distribution in the simulated chip very efficiently based on the proposed semi-analytical Green's function technique, which computes the Green's function online with only small overhead for building the Green's function library in prior for the given chip structure. Experimental results validate the accuracy of the semi-analytical Green's function. Our thermal analysis approach can adapt to the case that multi-layer heterogeneous heat conduction materials need be considered for the purpose of obtaining accurate thermal simulation results.

1. INTRODUCTION

The state of art integrated circuit design techniques make it popular that chips operate under several Gigahertz clock frequencies and integrate more than tens of millions of transistors. The resulted large power density induces considerable thermal problems. For reliability and performance consideration, much efforts need be spent in considering the more prominent electro-thermal effects during the design process. Fast thermal analysis tools which can provide accurate temperature profile for simulated chips would be much useful provided that the evaluation of thermal distribution can be done online efficiently.

There are two types of methods which much improved traditional thermal analysis procedures. They are the equivalent circuit network techniques using reduced order model representation [1] and free-space Green's function based approaches [2]. In this paper, focusing on the steady-state thermal simulation of integrated circuits and based on layered Green's function, we present a novel thermal analysis approach, which remains the fast speed advantage of free-space Green's function thermal analysis approach [2] and can directly handle multiple layer heterogeneous heat conduction materials in the thermal simulation procedure.

For structures consisting of homogeneous material, [3] presents very extensive derivations of Green's function for heat conduction problems. However, for integrated circuits, thermal analysis approaches using Green's function to handle multi-layer heterogeneous heat conduction materials are rarely seen. Layered Green's function for Poisson's differential equation has been studied in the area of electromagnetics [4] and fast computation methods for layered Green's function have been proposed and used for capacitance extraction [5]. In this paper, for heat conduction problem, we propose an accurate semi-analytical Green's function technique which

can be used for online calculation and also requires little overhead for characterizing the given chip structures in prior.

The rest of the paper is organized as follows: Section 2 presents the fast thermal analysis approach which includes the semi-analytical Green's function formulations and the temperature evaluation procedure using Green's function; Section 3 evaluates the efficiency and accuracy of the proposed thermal analysis approach; Section 4 concludes this work.

2. FAST THERMAL ANALYSIS APPROACH

The fast thermal analysis approach is based on layered Green's function, which measures the temperature response for a given heat source. The temperature distribution in integrated circuits is calculated by superposing the contributed temperature increments from all possible heat sources via Green's function.

2.1. Background

The heat conduction equation under rectangular coordinates is given as [3]

$$\nabla \cdot (\nabla T(x, y, z)) = -\frac{g(x, y, z)}{k(z)} \quad (1)$$

where T is temperature, $k(z)$ are the heat conductivity parameters, which only depend on the position on the Z axis, g denotes heat source. Here we omit the boundary conditions. Comparing the size of heat sources and the dimension of chip on the xy plane, we can assume the chip is infinite in the xy plane. Correspondingly, based on the resulted symmetry on radius ρ in cylinder coordinates, the Green's function $G(\rho, z)$ between points (ρ', z') and (ρ, z) for the heat conduction problem represented by (1) satisfies the following associated equation

$$\frac{\partial^2 G(\rho, z)}{\partial \rho^2} + \frac{1}{\rho} \frac{\partial G(\rho, z)}{\partial \rho} + \frac{\partial G(\rho, z)}{\partial z} = -\frac{\delta(\rho') \delta(z')}{2\pi \rho k(z)} \quad (2)$$

Using $\mathcal{G}(s, z)$, the Hankel transform of $G(\rho, z)$, given by

$$\mathcal{G}(s, z) \equiv \int_0^\infty G(\rho, z) \rho J_0(\rho s) d\rho$$

where $J_0(x)$ is the zero order Bessel function, and similarly applying the Hankel transform to (2), it can be obtained that

$$\frac{\partial^2 \mathcal{G}(s, z)}{\partial z^2} - s^2 \mathcal{G}(s, z) = -\frac{\delta(z')}{2\pi k(z)} \quad (3)$$

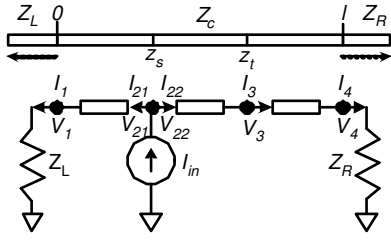


Fig. 1. Equivalent transmission line circuit: the case of objects in one layer

Compared (3) to the classic Telegrapher's equation for transmission line under impulse input given by

$$\frac{\partial^2 V}{\partial z^2} - r^2 V = -r Z_0 \delta(z') \quad (4)$$

where r is the propagation constant, $\delta(z')$ denotes the impulse input, and Z_0 is the characteristic impedance, the following analogy can be observed:

$$r \equiv s, \frac{1}{2\pi} \frac{V(r)}{r} \equiv G(s), Z_0 \equiv \frac{1}{k(z)}$$

As a result, we can make the following conclusion: defining the transfer impedance between the impulse input point z' and the observation point z as $Z(s)$ for the lossless transmission line with $R = G = 0$, $LC = 1$, and $\sqrt{\frac{L}{C}} = \frac{1}{k(z)}$, the Green's function for (1) in spatial domain between points (ρ', z') and (ρ, z) can be calculated using the following integral transform of $Z(s)$:

$$G(\rho, z) = \mathcal{H}[\rho, Z(s)] \equiv \frac{1}{2\pi} \int_0^\infty Z(s) J_0(\rho s) ds \quad (5)$$

The various types of boundary conditions: Dirichlet, Neumann and convection [3], can be incorporated into the equivalent equations for transmission line with short-circuited ends, open-circuited ends, or with appropriate load impedances.

2.2. Semi-analytical formulation of layered Green's function

The type of the integral transform denoted by (5) can be worked out conveniently through the numerical evaluation of transfer impedance and fast Hankel transform methods. However, on-line computation via such methods will be hard to be used due to the excessive computational time requirement. To ensure the efficiency of thermal analysis, we propose a semi-analytical technique for computing the layered Green's function from (5). It will be described in the following parts.

2.2.1. Evaluation of transfer impedance

First we formulate the $Z(s)$ in (5) for objects in one layer. Fig. 1 shows the equivalent transmission line circuit, which consists of one uniform transmission line with two loads. The transfer impedance $Z(s)$ between source point z_s and target point z_t can be obtained as

$$Z(s) = \frac{V_3(s)}{I_{in}(s)} = \sum_{i,j \in \{1,2\}} B_{ij}(s) K_{ij}^s(z_s, l - z_t) \quad (6)$$

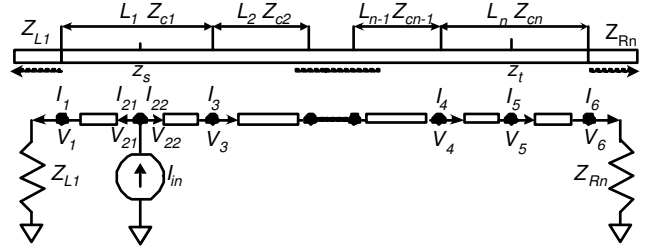


Fig. 2. Equivalent transmission line circuit: the case of objects in multiple layers

where

$$B_{ij}(s) = \frac{Z_c [Z_L(s) + (-1)^i Z_c] [Z_R(s) + (-1)^j Z_c]}{C(s)}$$

$$C(s) = Z_c [Z_L(s) + Z_R(s)] \cosh[sl] + [Z_L(s) Z_R(s) + Z_c^2] \sinh[sl]$$

Z_c is the transmission line characteristic impedance, $K_{ij}^s(p, q)$ is named as kernel ij in the rest of the paper, defined as

$$K_{ij}^s(p, q) \equiv \frac{\exp\{s[(-1)^i p + (-1)^j q]\}}{4}$$

Now we formulate the $Z(s)$ in (5) for objects in multiple layers. Fig. 2 shows the equivalent transmission line circuit, where several transmission line segments with different characteristic impedances are connected together to represent the multi-layer heterogeneous heat conduction materials in the z direction. The transfer impedance $Z(s)$ between the input of port 2 and port 5 can be obtained as

$$Z(s) = \frac{V_5(s)}{I_{in}(s)} = \sum_{i,j \in \{1,2\}} D_{ij}(s) K_{ij}^s(z_s, l_n - z_t) \quad (7)$$

where $D_{ij}(s) = \frac{Z_{c1} Z_{R1}(s) [Z_{L1}(s) + (-1)^i Z_{c1}] [Z_{Rn}(s) + (-1)^j Z_{cn}]}{E(s)}$ with

$$E(s) = F(s) \{ Z_{c1} [Z_{L1}(s) + Z_{R1}(s)] \cosh[sl_1] + [Z_{c1}^2 + Z_{L1}(s) Z_{R1}(s)] \sinh[sl_1] \} \cdot \{ Z_{Rn}(s) \cosh[sl_n] + Z_{cn}(s) \sinh[sl_n] \} \quad (8)$$

$$F(s) = \prod_{2 \leq k \leq n-1} \left(\cosh[sl_k] + \frac{Z_{ck}}{Z_{Lk}} \sinh[sl_k] \right)$$

In the above, Z_{Lk} and Z_{Rk} are the input impedance of port k to the left and right side respectively, and Z_{ck} is the characteristic impedance of transmission line segment k . The input impedance $Z_{in}(s)$ to either side of the transmission line can be calculated recursively via the following formula:

$$Z_{in}(s) = Z_c \frac{Z'_{in} + Z_c \tanh[sl]}{Z_c + Z'_{in} \tanh[sl]} \quad (9)$$

where Z'_{in} is the input impedance defined for the next transmission line segment. l is the transmission line length.

2.2.2. semi-analytical formulation of Green's function

In this part, we present the semi-analytical Green's function technique. By using the modified Prony's algorithm [6], the coefficient functions $f(s)$, i.e. $B_{ij}(s)$ and $D_{ij}(s)$ in the derived transfer impedance representation (6) and (7) are approximated by summing a set of exponential functions, given as

$$f(s) \approx \sum_{k=1}^m c_k e^{s d_k} \quad (10)$$

In the actual fitting procedure using modified Prony's algorithm, a set of weighting coefficients can be applied to the square error function in order to improve the accuracy of Green's function for radiuses in certain region. For instance for far fields, the weighting matrix can be constructed using the envelop of the zero order Bessel function which damps in terms of $1/\sqrt{\rho}$, where ρ is the input parameter for the Bessel function. The B matrix in [6] incorporating the weighting matrix W is derived as

$$\begin{aligned} B_{ij} &= y^T X_i A X_j^T y - y^T X A X_i^T W^{-2} X_j A X^T y \\ A &= X^T W^{-2} X \end{aligned} \quad (11)$$

From (6), (7) and (10), the transfer impedance function $Z(s)$ between z_s and z_t can be represented accordingly as

$$Z(s) \approx \sum_{i,j \in \{1,2\}} K_{ij}^s(z_s, l_t - z_t) \sum_{k=1}^m c_{ijk} \exp[s d_{ijk}] \quad (12)$$

where l_t is the length of the transmission line in which the target point z_t lies. We will name d_{ij} , the union of d_{ijk} , as the set of modes indexed by ij in the rest of the paper. For the integral transform defined by (5), it can be verified that

$$\mathcal{H}[\rho, e^{s d} K_{ij}^s(p, q)] = \frac{1}{\sqrt{[d + (-1)^i p + (-1)^j q]^2 + \rho^2}} \quad (13)$$

for $d \leq (-1)^i p + (-1)^j q$

The semi-analytical technique for computing layered Green's function is summarized in the follows. The coefficients in representation (10), which are *independent* on the positions of source and observation points, are pre-calculated and tabulated for only those combinations of layers exist interactions. Although the worst-case space complexity is $O(N^2)$, where N is the number of layers, the space usage is still very small since the number of layers is not so big. Using the tabulated coefficients, the Green's function between any source and observation points can be calculated on-line efficiently via (12) and (13).

Since the semi-analytical Green's function method need not use interpolation from known Green's function to obtain Green's function in unknown locations, it avoids storing many sampling of Green's function in different locations and reduces the space requirement compared to methods using numerical interpolation. Also the proposed approach uses simple calculus by (13) instead of Hankel transform method and improves the computation efficiency. In addition, modified Prony's algorithm using weighting matrices by the derived formula in (11) can be used to improve the accuracy of Green's function in specific regions.

2.3. Thermal analysis via Green's function

In the proposed fast thermal analysis method, the temperature for a location is obtained by summing up the contribution from each heat source using the semi-analytical Green's function.

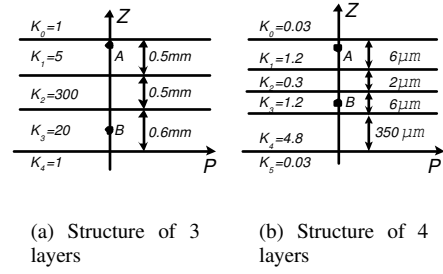


Fig. 3. The two simulated multi-layer structures

From (13), the temperature increments $\Delta T(x_0, y_0, z_0)$ at point $W(x_0, y_0, z_0)$ resulting from heat sources can be calculated by

$$\begin{aligned} \Delta T(x_0, y_0, z_0) &= \sum_{hs \in U} dens(hs) \Delta T^{hs}(x_0, y_0, z_0) \\ \Delta T^{hs}(x_0, y_0, z_0) &= \sum_{i,j \in \{1,2\}} \sum_{d \in d_{ij}} T_{ij}^d \end{aligned} \quad (14)$$

For the case hs and W in multiple layers:

$$T_{ij}^d = I_{i,j}^d(z_1, z_2, l_0 - z_0)$$

For the case hs and W in single layer:

$$T_{ij}^d = \begin{cases} I_{i,j}^d(z_1, z_0, l_0 - z_0) \\ + I_{j+1,i}^d(z_0, z_2, z_0 + (-1)^{(j-i)} l_0), & z_1 \leq z_0 \leq z_2 \\ I_{j+1,i}^d(z_1, z_2, z_0 + (-1)^{(j-i)} l_0), & \text{otherwise} \end{cases}$$

In the above, U denotes the union of all objects, $\Delta T^{hs}(x_0, y_0, z_0)$ denotes the temperature increments caused by object hs , $dens(hs)$ denotes the power density of hs , d_{ij} is the set of modes indexed by ij for the pair of layers where hs and $W(x_0, y_0, z_0)$ locate respectively, l_0 is the height of the layer where W locates, the position and dimension of object hs are determined by $x_1 : x_2, y_1 : y_2$ and $z_1 : z_2$, and $I_{p,q}^d(z_a, z_b, z_c)$ is the integral defined as

$$I_{p,q}^d(z_a, z_b, z_c) = \int_{x_1}^{x_2} \int_{y_1}^{y_2} \int_{z_a}^{z_b} \frac{dxdydz}{\sqrt{[d + (-1)^p z + (-1)^q z_c]^2 + (x-x_0)^2 + (y-y_0)^2}} \quad (15)$$

3. EXPERIMENTAL RESULTS

As can be seen from (5), (6) and (7), the Green's function only depends on the relative heat conductivity of each layer, and can be scaled linearly with respect to the unit of the height of each layer. This facilitates us to evaluate the accuracy of the semi-analytical Green's function. All positions in z axis are given here in terms of intra-layer positions. Fig. 3 shows two multi-layer structures consisting of heterogeneous heat conduction materials. Fig. 4 compares the results of using the semi-analytical Green's function method and direct numerical integration method for the structure shown in Fig. 3(a), where k_i indicates the heat conductivity, k_0 and k_4 represent the heat conductivity of free space. In Fig. 4, SXXYY corresponds to the Green's function between the observation plane and source point locating at the Same layer, where XX denotes the source point at $z = XX * UNIT$, YY denotes the observation plane at $z = YY * UNIT$ and $UNIT =$

ρ mm	S11	2148	M13	2148	S11	0135	M13	0135
0	70.5	69.4	8.23	8.4	72.2	72.4	10.1	10.4
0.1	67.1	66.1	8.2	8.36	69.6	69.6	10.1	10.8
0.2	59.4	58.6	8.13	8.26	63.0	62.8	10.0	10.2
0.3	51.1	50.6	8.01	8.11	55.2	54.7	9.82	10.0
0.4	43.8	43.6	7.84	7.9	47.6	47.2	9.59	9.73
0.5	37.8	37.6	7.64	7.66	41.1	40.6	9.31	9.38
0.6	32.9	32.7	7.41	7.39	35.6	35.2	8.99	9.0
0.7	28.8	28.6	7.16	7.11	31.0	30.7	8.64	8.6
0.8	25.4	25.2	6.9	6.82	27.2	26.9	8.28	8.2
0.9	22.6	22.3	6.64	6.53	24.1	23.8	7.9	7.79
1.	20.2	19.9	6.37	6.25	21.4	21.1	7.53	7.4

Table 1. The Green’s function for the structure shown by Fig. 3(b)

$10\mu\text{m}$, and MXXYY corresponds to the Green’s function between source point in layer 1 and observation plane in layer 3. The plotted symbols denote the numerical integration results, and the lines denote results using the semi-analytical Green’s function method. The percentages (**not in logarithmic scale**) shown in the legend are the maximum error percentages between the two methods, from which we can see that the semi-analytical Green’s function method is very accurate, for instance for S0149, the maximum error percentage between the results of the two methods for the radiuses from 0 to 1.2mm is only 0.59%.

Table 1 shows the Green’s function for the structure in Fig. 3(b). In the table, the data in two adjacent columns show the comparison, where S11 or M13 columns are results of the semi-analytical Green’s function method, 11 denotes both source point and observation plane in layer 1, 13 denotes source point in layer 1 and observation plane in layer 3, columns labelled by XXYY, which has the same meaning as that in Fig. 4 except $UNIT = 0.1\mu\text{m}$, are the numerical integration results. The accuracy of the semi-analytical Green’s function method is also verified by the table.

The advantage of the semi-analytical Green’s function technique can be observed since we only characterize the structure once to obtain the coefficients in (10). The obtained coefficients are fixed when the source point and observation plane changes. Typically each coefficient function is approximated using not more than 7 modes, and the space requirement for storing these coefficients is negligible. The online calculation is done very efficiently by using (13) with these fixed coefficients.

Fig. 5 shows the thermal simulation results for the structure shown in Fig. 3(b) by using the formulas and procedures in Section 2.3. The hot-spots in the two planes can be easily identified from the two figures. The hot-spots also imply the locations of heat sources in the two layers.

4. CONCLUSIONS

In this paper, we present a novel thermal analysis approach based on the proposed accurate and efficient semi-analytical Green’s function method. We derive the formulas used in the evaluation of Green’s function and temperature distribution. The proposed thermal analysis method is a promising approach when heterogeneous heat conduction materials need be considered for the purpose of conducting accurate thermal analysis.

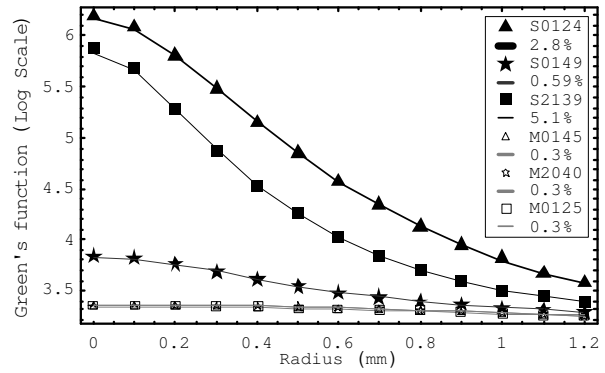


Fig. 4. Evaluating the accuracy of semi-analytical Green’s function for the structure shown by Fig. 3(a)

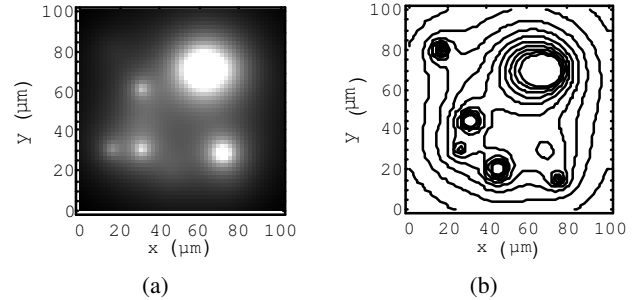


Fig. 5. Temperature distribution in layer 1 and layer 3 for the structure in Fig. 3(b): (a) Plot of temperature intensity in layer 1 at $z=3\mu\text{m}$; (b) Isothermal contour plot of temperature in layer 3 at $z=3\mu\text{m}$.

5. REFERENCES

- [1] L. Codecasa, D. D’Amore, and P. Maffezzoni, “An arnoldi based thermal network reduction method for electro-thermal analysis,” *IEEE Trans. Comp., Packag., Manufact. Technol. A*, vol. 26, pp. 186–192, Mar. 2003.
- [2] M. S. Yee and L. Hanzo, “An efficient method for hot-spot identification in ulsi circuits,” in *Proc. IEEE/ACM International Conference on Computer-Aided Design ’99*, Nov. 7–11, 1999, pp. 124–127.
- [3] J.V.Beck, K. Cole, A. Haji-Sheikh, and B. Litkouhi, *Heat Conduction Using Green’s Functions*. Hemisphere, 1992.
- [4] R. Crampagne, M. Ahmadpanah, and J.-L. Guiraud, “A simple method for determining the green’s function for a large class of mic lines having multilayered dielectric structures,” *IEEE Trans. Microwave Theory Tech.*, vol. 26, pp. 82–87, Feb. 1978.
- [5] J. Zhao, W. Dai, S. Kadur, and D. Long, “Efficient three-dimensional extraction based on static and full-wave layered green’s functions,” in *Proc. IEEE/ACM Design Automation Conference ’98*, June 15–19, 1998, pp. 224–229.
- [6] M. R. Osborne and G. K. Smyth, “A modified Prony algorithm for exponential function fitting,” *SIAM Journal on Scientific Computing*, vol. 16, no. 1, pp. 119–138, 1995.